ELSEVIER

Surface Science 513 (2002) 211–220

SURFACE SCIENCE

www.elsevier.com/locate/susc

First-principles calculations for $SrTiO_3(100)$ surface structure

E. Heifets [a,*], R.I. Eglitis [b], E.A. Kotomin [c,d], J. Maier [c], G. Borstel [b]

[a] *California Institute of Technology, 7720 W. Hampton Avenue, #211, MS 139-74, Pasadena CA 91125, USA*
[b] *Fachbereich Physik, Universität Osnabrück, D-49069 Osnabrück, Germany*
[c] *Max Planck Institut für Festkörperforschung, Heisenbergstr. 1, D-70569 Stuttgart, Germany*
[d] *Institute for Solid State Physics, University of Latvia, 8 Kengaraga str., Riga LV-1063, Latvia*

Received 8 January 2002; accepted for publication 9 April 2002

Abstract

As a continuation of our recent ab initio calculations of $SrTiO_3(100)$ surface relaxation for the two different terminations (SrO and TiO_2) [Phys. Rev. B 64 (2001) 23417], we analyze here their electronic structures (band structure, density of states, and the electronic density redistribution with emphasis on the covalency effects). We compare results of ab initio Hartree–Fock method with electron correlation corrections and density functional theory with different exchange-correlation functionals, including hybrid (B3PW, B3LYP) exchange techniques. Our results are also compared with previous ab initio plane-wave local density approximation calculations and experiments when available. Considerable increase of Ti–O chemical bond covalency nearby the surface and the gap reduction, especially for the TiO_2 termination, are confirmed.

Keywords: Single crystal surfaces; Surface relaxation and reconstruction; Surface structure, morphology, roughness, and topography; Ab initio quantum chemical methods and calculations

1. Introduction

Thin films of ABO_3 perovskite ferroelectrics are important for many applications [1–3]. In particular, the titanates are interesting materials concerning their electrochemical properties and promising conductors for, e.g. electrodes and sensors. Surface properties of $SrTiO_3$ are important for catalysis and for epitaxial growth of high T_c superconductors. For all these applications surface structure and its quality are of primary importance. Several ab initio [4–10] and shell model [11–13] studies were published for the (100) surface of $BaTiO_3$ and $SrTiO_3$ crystals.

Recently [14], we also calculated the relaxed atomic structure of the $SrTiO_3(100)$. The main motivation was to study in a regular way the dependence of the surface relaxation properties upon the choice of exchange-correlation functionals and localized/plane-wave basis sets used in different calculations. One of our main conclusions was that all methods irrespective on the particular exchange-correlation functional, agree quite well on both surface energies and on atomic displacements nearby the surface. The $SrTiO_3(100)$ surface relaxation and rumpling have been studied also experimentally, by means of several techniques (for more references see [4,10,14]). Theory agrees with

* Corresponding author. Tel.: +1-3238512724.
E-mail address: heifets@wag.caltech.edu (E. Heifets).

0039-6028/02/$ - see front matter
PII: S0039-6028(02)01730-2

LEED, RHEED experiments on the larger rumpling for the SrO termination. However, there is a disagreement about direction of surface O atom displacement on the TiO_2-terminated surface, probably, due to neglect in theory of the anharmonic vibrations of the surface atoms, especially Ti. On the other hand, several diffraction experiments clearly contradict each other, very likely, due to difference in sample preparations and as a result of the different interpretations of indirect experimental data on the atomic relaxation at the surface [4].

In this paper, we analyze the *electronic structure* of the $SrTiO_3$ surfaces. This is motivated by the conclusion about enhanced Ti–O covalent bonding near surface [15] which we wanted to check, and the UPS spectra measured for the two terminations [16].

2. Method

Since we discuss experiments performed at room temperature, in this study we continue simulations of $SrTiO_3$ surfaces [23] for the cubic perovskite phase stable above 105 K. The strontium titanate unit cell in this phase is shown in Fig. 1a. To simulate (0 0 1) surfaces, we used symmetrical slabs consisting of seven alternating TiO_2 and SrO layers. One of these slabs was terminated by SrO planes. The second slab was terminated by TiO_2 planes. These two terminations are the only two possible flat and dense (0 0 1) surfaces in perovskite lattice structure. The structure of these slabs is illustrated in Fig. 1b and c.

The total energies and electronic structures of the TiO_2- and SrO-terminated slabs were calculated using several quite different methods: Hartree–Fock (HF) with different density functional theory (DFT)-type a posteriori electron correlation corrections to the total energy [17] such as generalized gradient approximation (HFGGA), Perdew-91 (HFPer91), Lee, Yang, Parr (HFLYP); and full-scale DFT calculations based on the Kohn-Sham equation with a number of exchange-correlation functionals, including local density approximation (LDA), generalized gradient approximations (GGA) by Perdew and Wang (PW), Perdew, Burke and Ernzerhof (PBE), as well as Becke exchange functional with Lee–Yang–Parr correlation functional (BLYP). We used also the so-called *hybrid* HF–DFT exchange functionals, in which HF exchange was mixed with DFT exchange functionals using Becke's three-parameter method, combined with the non-local correlation functionals by Perdew and Wang (B3PW), as those by Lee, Yang, and Parr (B3LYP). For all calculations, we used the CRYSTAL-98 computer code (see [18] and references therein for description of all techniques mentioned), in which both (HF/DFT) types of calculations are implemented on equal grounds. Unlike previous plane-wave calculations, this code uses the localized Gaussian-type basis set. In our simulations we applied the standard basis set recommended for $SrTiO_3$ [18]. Another advantage of the CRYSTAL-98 code is its treatment of purely 2D slabs, without an artificial periodicity in the direction perpendicular to the surface, commonly employed in all previous surface band-structure calculations (e.g., [4,10]). Detailed analysis of the optimized atomic structure was presented in Ref. [14].

In this study we analyze the band structure, total and projected density of states (DOS), bond populations, and the atomic charges, dipoles and quadrupole moments In particular, the quadrupole $q(20)$ moments characterize atomic deformation and polarization along the z axis perpendicular to the surface [14,18].

3. Main results

3.1. Bulk properties

Table 1 presents results for the effective static (Mulliken) charges and atomic quadrupoles in the $SrTiO_3$ bulk. The effective charges for Ti and O ions, both in the bulk and on the surface, are much smaller than formal ionic charges ($4e$, $-2e$, respectively). This arises due to the partly covalent nature of the Ti–O chemical bond. In contrast, Sr charge remains close to the formal charge, $+2e$. Note that the results are similar for all methods used, ranging from HF to DFT-LDA. The Ti–O chemical bond covalency is confirmed by the bond

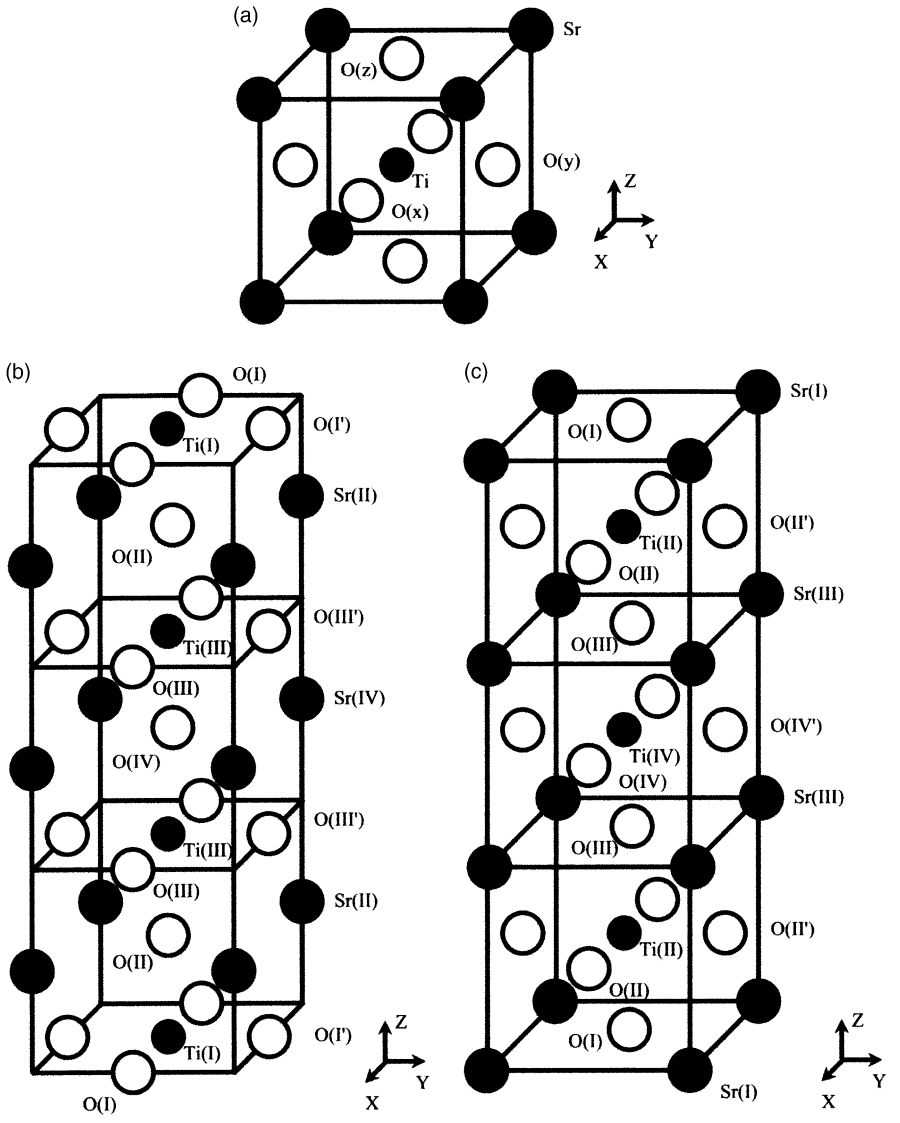

Fig. 1. Schematic sketch of (a) unit cell for cubic perovskite structure of the bulk $SrTiO_3$, (b) unit cell for TiO_2-terminated seven-layers slab of $SrTiO_3$, (c) that for SrO termination. Atomic numbering introduced in this figure is used in Tables 2–4.

Table 1
Effective charges and quadrupole moments of atoms calculated for the bulk $SrTiO_3$ by means of variety of DFT and HF methods

Atom (A)	Charge Q, quadrupole q	LDA	B3LYP	B3PW	BLYP	PBE	PWGGA	HF
Sr^{2+}	Q, e	1.83	1.85	1.85	1.84	1.83	1.83	1.91
Ti^{4+}	Q, e	2.13	2.33	2.27	2.27	2.21	2.21	2.58
$O^{2-}(z)$	Q, e	−1.32	−1.39	−1.38	−1.37	−1.35	−1.35	−1.50
	$q(2,0)$, e AU^2	0.83	0.64	0.66	0.61	0.64	0.65	0.60

Table 2
Bond populations (in me) for the bulk $SrTiO_3$ (negative populations mean atomic repulsion)

Atom A	Atom B	LDA	B3LYP	B3PW	BLYP	PBE	PWGGA	HF
O(z)	O(x)	−48	−36	−36	−30	−32	−34	−40
	Sr	−10	−8	−10	−4	−6	−6	−10
	Ti	52	74	82	66	74	70	112

populations in Table 2, which slightly varies, dependent on the particular method. Obviously, there is no chemical bonding between any other types of atoms, e.g. Sr–O or O–O. As is well known, the Mulliken effective charges are basis dependent, this is why the trend is more important than the absolute charges. Both effective atomic charges and bond populations (Tables 1 and 2) increase in a series of DFT functionals, which increasingly better account for the exchange effects, i.e. LDA-GGA-hybrid functionals and lastly, HF. The optical band gap usually also increases in the same series. Since vacant orbitals in $SrTiO_3$ are localized on cations, an increase of the band gap leads to an additional transfer of the electron density from cations to anions, accompanied by a growth of ionicity.

We have analyzed different contributions to the Ti–O bond population. It appears that the Ti–O bond population has two contributions: a positive contribution due to chemical bonding of 2p-orbitals of O ions with 4d-orbitals of Ti, and a negative contribution as result of repulsion of the same orbitals of O ions from Ti ion *cores* (both s- and p-orbitals). The positive contribution (chemical bonding) does not change much in a series of calculations with different exchange-correlation functionals. However, the negative contribution decreases significantly, which results in an increase of the total bond population.

Large quadrupole $q(20)$ moments in Table 2 confirm the considerable deformation of O atoms caused by the chemical bonding with Ti atoms.

3.2. Charge distribution near the surface

The effective atomic charges (calculated by using the standard Mulliken population analysis), dipole and quadrupole atomic moments for SrO and TiO_2 terminations were discussed in Ref. [14]. For all methods used the cation charges in the two top layers in the SrO-terminated surface turned out to be smaller than in the bulk. In contrast, the O negative charges in these layers became even more negative, due to additional electron charge transfer. Changes in atomic charges in deeper layers become very small, their sign vary, dependent on the used exchange-correlation functional. These effects are pronounced more strongly in the case of TiO_2-terminated surface. In particular, charge reduction of surface Ti ions ($-0.13e$) is much larger than that on the SrO-terminated surface ($-0.03e$). Charges of Sr ions in the subsurface layer of TiO_2-terminated surface are close to Sr charges in the top layer of SrO-terminated surface. In the third layer Ti charges are still reduced, but the magnitude of the charge reduction is relatively small. Sr charges in the central layer of the slab are essentially the same as in the $SrTiO_3$ bulk. In contrast, the O charges are reduced through the entire TiO_2-terminated slab. This O charge reduction is especially large in the top two layers nearby the surface.

The *differences* in the charge densities at [0 0 1] planes in the $SrTiO_3$ bulk and on the (0 0 1) surfaces for both terminations are analyzed in Table 3. This is quite usual that ionic charges obtained in quantum-mechanical computations are smaller than formal ionic charges and our calculations is not an exception. As a result, [0 0 1] planes in the bulk turn out to be *charged*, with a charge density per unit cell $\sigma_B(SrO) = -\sigma_B(TiO_2)$ (see Table 3(panel A)). A half of this charge density is donated from the TiO_2 planes to each of the two neighboring SrO planes. If the charge densities of these planes were calculated using formal ionic charges, they would be neutral. This charge redistribution makes the (0 0 1) surfaces to be *polar*, with the dipole moment perpendicular to the surface. (In our slab model this moment disappear

Table 3
Charge densities in the (0 0 1) crystalline planes of the bulk $SrTiO_3$ (in e, per TiO_2 or SrO unit) (panel A); charge density and its change with respect to the bulk (in brackets) in four top planes (I to IV) of the TiO_2-terminated (0 0 1) slab (panel B); charge density and its change (in brackets) in four top planes of the SrO-terminated (0 0 1) slab (panel C)

Unit	Charge	LDA	B3LYP	B3PW	BLYP	PBE	PWGGA	HF
Panel A								
TiO_2	$Q(e)$	−0.51	−0.46	−0.48	−0.47	−0.49	−0.49	−0.41
SrO	$Q(e)$	0.51	0.46	0.48	0.47	0.49	0.49	0.41
Panel B								
TiO_2(I)	Q, e	−0.34 (0.17)	−0.32 (0.14)	−0.32 (0.16)	−0.33 (0.14)	−0.33 (0.16)	−0.32 (0.16)	−0.28 (0.13)
SrO(II)	Q, e	0.58 (0.06)	0.53 (0.07)	0.54 (0.06)	0.54 (0.07)	0.54 (0.06)	0.55 (0.07)	0.47 (0.06)
TiO_2(III)	Q, e	−0.49 (0.02)	−0.44 (0.02)	−0.46 (0.02)	−0.44 (0.02)	−0.46 (0.03)	−0.47 (0.02)	−0.40 (0.01)
SrO(IV)	Q, e	0.51 (0.00)	0.46 (0.00)	0.48 (0.00)	0.47 (0.00)	0.49 (0.00)	0.49 (0.00)	0.42 (0.01)
Panel C								
SrO(I)	Q, e	0.45 (−0.06)	0.37 (−0.09)	0.39 (−0.09)	0.36 (−0.11)	0.39 (−0.10)	0.38 (−0.10)	0.32 (−0.09)
TiO_2(II)	Q, e	−0.71 (−0.20)	−0.59 (−0.13)	−0.61 (−0.13)	−0.57 (−0.10)	−0.61 (−0.13)	−0.61 (−0.13)	−0.50 (−0.09)
SrO(III)	Q, e	0.52 (0.01)	0.45 (−0.01)	0.46 (−0.02)	0.45 (−0.01)	0.47 (−0.01)	0.48 (−0.01)	0.40 (−0.01)
TiO_2(IV)	Q, e	−0.51 (0.01)	−0.47 (−0.01)	−0.48 (−0.01)	−0.48 (−0.01)	−0.49 (−0.01)	−0.49 (−0.01)	−0.42 (−0.01)

due to the symmetry plane.) This is also called "type-III surface", according to generally accepted classification by Tasker [19], instead of a neutral, or "type-I surface".

Since we neglect defect creation in this study, the only way to stabilize this surface is to add the compensating charge density $\sigma_B/2$ to the TiO_2-terminated surfaces and $-\sigma_B/2$ to the SrO-terminated surfaces. This additional charge density coincides with the density, which was transferred from the TiO_2[0 0 1] plane to each of its neighboring SrO planes.

The charge density changes with respect to the bulk properties are summarized in Table 3(panels B and C) (numbers in brackets). As one can see, the additional charge is mostly localized on the TiO_2 unit in the first or second plane, dependent on the termination. This is true for all exchange-correlation functionals used for TiO_2 termination, and for most functionals for the SrO termination (except for BLYP and HF). In the latter case the additional charge located at the top SrO layer just a little bit exceeds the additional charge at the subsurface TiO_2 layer. All above-described charge redistribution is in line with ideas of a *weak polarity* [20]. Ion polarization at surfaces with both terminations is significant in the top two planes and becomes very small in deeper layers.

On the SrO-terminated surface *both* Sr and O ions have negative dipole moments. This means that their dipole moments are directed inwards to the surface (direction outwards from the surface is chosen as positive). The dipole moments of Sr ions are surprisingly large, only by ~30% less then those for surface oxygen ions. In the subsurface layer of SrO-terminated surface Ti atoms also reveal considerable negative dipole moments. These moments are smaller than those of the surface cations by 55–65%. Polarization of Sr ions in the third layer is very small, but still found negative for all used functionals. Polarization of O ions in the subsurface layer, as well as in the next third layer, is also insignificant. For most functionals used, the O dipole moments in these layers are negative. The only exception are calculations with LDA and B3LYP functionals giving the positive dipole moments for the subsurface O ions, and LDA calculations for O ions in the third layer. However, these effects are very delicate since dipole moments are very small.

On the TiO_2-terminated surface polarization of cations has an opposite sign than on the SrO-terminated surface: surface Ti ions now reveal positive dipole moments. The polarization value is approximately the same but with an opposite sign as compared with subsurface Ti for the SrO termination. Dipole moments on the subsurface Sr ions are small but also positive. In the third layer the dipole moments on Ti ions turn out to become negative (for all methods except HF calculations).

Oxygen polarization on the TiO_2-terminated surface is surprisingly small.

In the surface layer calculated O dipole moments are negative for most functionals, except for PBE and PWGGA. These moments become positive on the subsurface O ions and, again, negative on the O ions in the third layer.

Bond populations between atoms for the TiO_2 termination are given in Table 4. Let us, for the analysis, assume the TiO_2 termination and look at the particular B3PW results. The major effect observed here is strengthening of the Ti–O chemical bond near the surface (compare with the bulk, where the Ti–O bond is considerably populated with 82 me, m = milli). The Ti–O bond population for the TiO_2-terminated surface is 128 me, which is considerably larger than the relevant values in the bulk. The Ti–O populations in the direction perpendicular to the surface, i.e. between Ti and O atoms in the first and second, the second and third plane, and lastly, the third and fourth planes (124, 92, and 86 me) also exceed the bulk value. In contrast, the Sr–O and O–O populations are very small and even negative, what indicates the atomic repulsion. This is supported by the Sr effective charges, which are close to the formal ionic charge of $+2e$. All these observations based on the effective charges and bond populations, agree well with analysis of the electronic density maps discussed earlier [14].

3.3. Band structure and DOS

Fig. 2 presents the band structure of the bulk, TiO_2 and SrO-terminated surfaces calculated by means of the hybrid B3PW method. These band structures are similar to results of previous ab initio plane-wave calculations [4]. The values of direct and indirect optical gaps are summarized in Table 5. The total and projected DOS for the bulk material are plotted in Fig. 3, whereas Figs. 4 and 5 show DOS for TiO_2- and SrO-terminated slabs, respectively.

The upper valence band for the $SrTiO_3$ bulk (Fig. 2a) is quite flat, with the top at M and R points of the Brillouin zone, and almost perfectly flat upper valence band between these points. The bottom of the lowest conduction band lies at the Γ point, with very close energy to the X point. The dispersion curve between these Γ and X points is very flat. Such flat bands could make possible hole and exciton self-trapping. An exciton self-trapping in $SrTiO_3$ bulk was indeed discussed quite recently [21].

Table 4
Atomic bond populations for the TiO_2 termination (numbers indicate the plane number from the surface)

Atom A	Atom B	LDA	B3LYP	B3PW	BLYP	PBE	PWGGA	HF
O(I)	O(I)	−36	−28	−30	−24	−26	−26	−34
	Ti(I)	108	124	128	114	118	114	146
	Sr(II)	−10	−10	−10	−4	−4	−6	−28
	O(II)	−20	−16	−16	−10	−8	−10	−36
O(II)	Ti(I)	100	132	124	128	120	118	150
	O(II)	4	2	2	2	2	2	2
	Sr(II)	−8	−8	−10	−4	−4	−6	−20
	Ti(III)	78	92	92	84	86	88	104
	O(III)	−38	−30	−32	−24	−24	−26	−42
O(III)	Sr(II)	−4	−4	−6	0	−2	−2	−18
	O(III)	−42	−34	−36	−30	−30	−32	−44
	Ti(III)	62	86	86	76	78	74	114
	Sr(IV)	−8	−8	−10	−4	−4	−6	−22
	O(IV)	−46	−36	−34	−30	−18	−20	−44
O(IV)	Ti(III)	54	78	80	68	72	70	106
	O(IV)	4	2	2	2	2	2	2
	Sr(IV)	−10	−8	−10	−4	−30	−6	−22

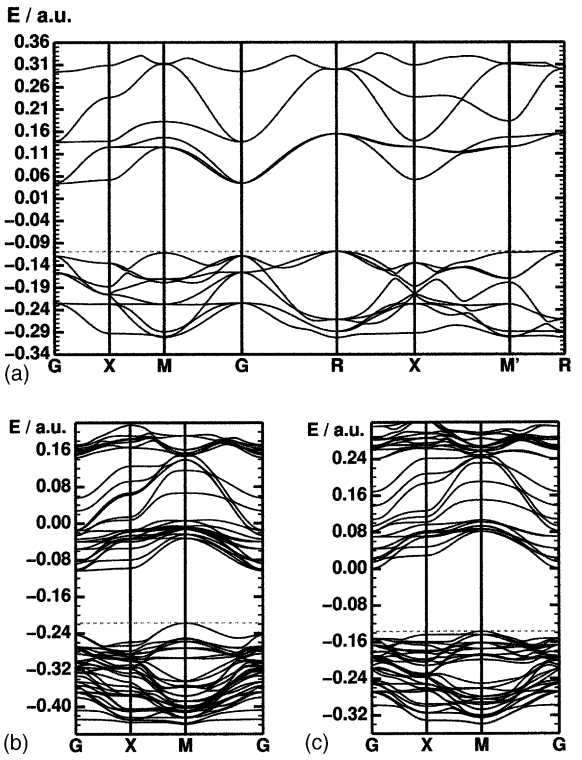

Fig. 2. The band structure of $SrTiO_3$ bulk (a), TiO_2- (b) and SrO-terminated (c) surfaces. B3PW calculations were performed for the symmetric seven-layer slabs. Calculation of the surface Brillouin Zone corresponds to the square 2D lattice.

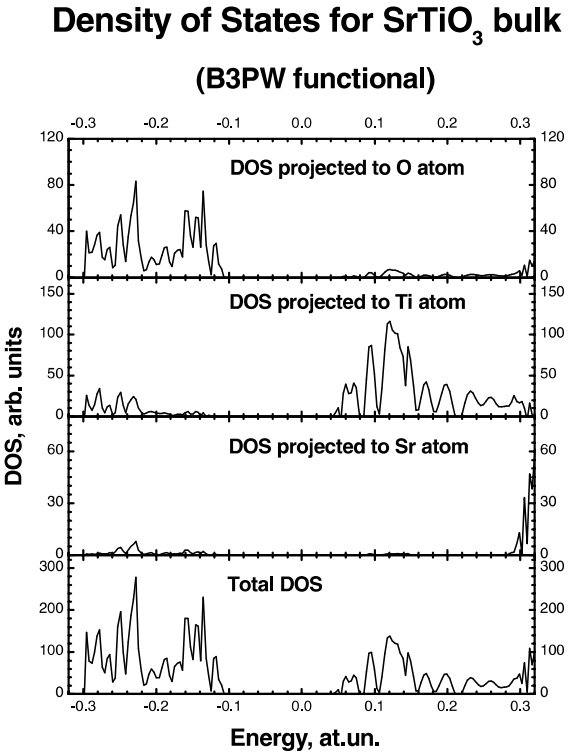

Fig. 3. Total and projected DOS for the bulk $SrTiO_3$.

The optical bulk gap obtained with the hybrid B3PW method is 4.16 eV, to be compared with the experimental value of 3.3 eV. This corresponds to much better agreement than in the case of typical considerable overestimate of the gap in "pure" HF calculations, or great underestimate in LDA calculations (1.85 eV [4]). The upper valence band consists of O 2p atomic orbitals with a small admixture of orbitals of Ti atoms, whereas conduction band bottom consists essentially of Ti orbitals. Orbital contribution from Sr atoms is negligible in this energy range. The Sr orbitals make a significant contribution to the DOS only at energies much higher in the conduction band.

The top of the upper valence band for the TiO_2-terminated slab is located at the M point of the Brillouin zone (Fig. 2b). At this point the valence band is split off about 1 eV from other valence bands. Analysis of contributions to the DOS shows that this band consists mainly of orbitals belonging to the surface O ions and can be considered as a

Table 5
The calculated B3PW optical gap (in eV) for the bulk and surface-terminated $SrTiO_3$ [2]

	Direct gap				Indirect gap	
	Γ	X	M	R	$M-\Gamma$	$R-\Gamma$
Bulk	4.43	5.08	6.45	7.18	4.23	4.16
SrO	4.12	4.70	5.94		3.71	
TiO_2	3.78	4.38	5.04		3.09	

Experimental bulk gap is 3.3 eV.

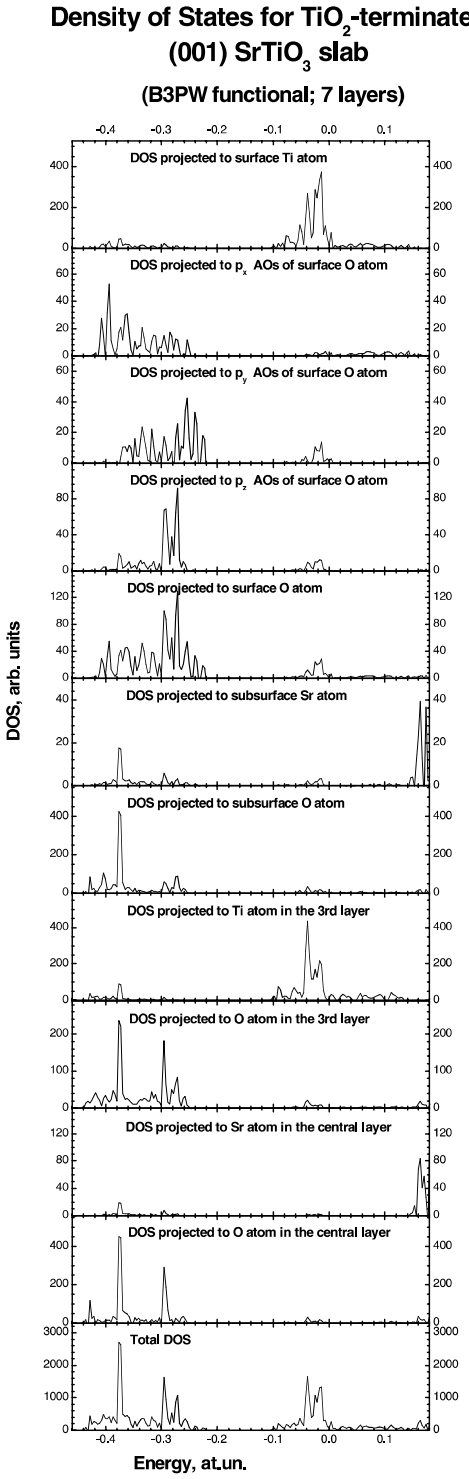

Fig. 4. The DOS for TiO_2-terminated surfaces.

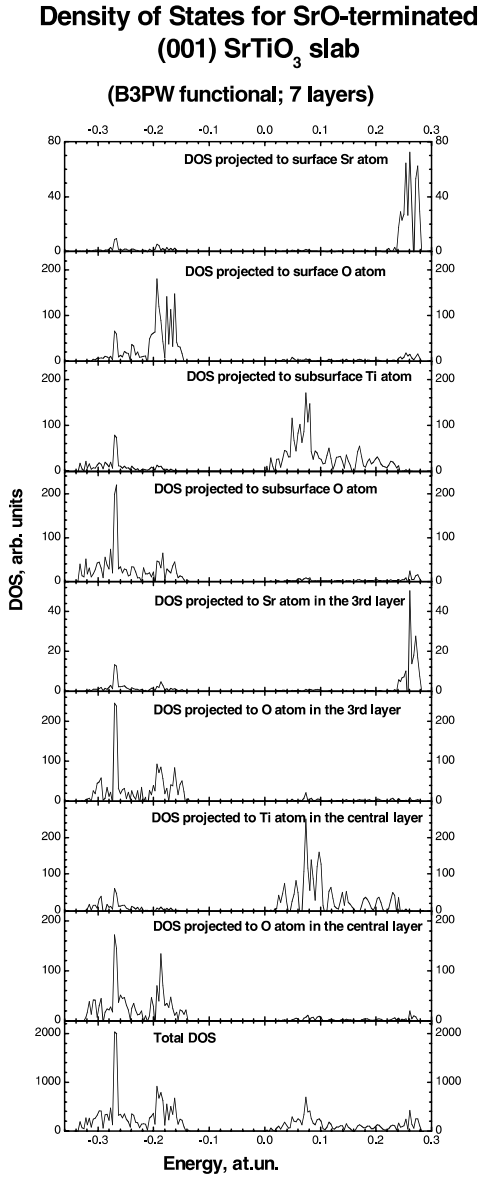

Fig. 5. The DOS for SrO-terminated surfaces.

band of surface states. For a more detailed study of the surface O atom contribution to the DOS we calculated DOS projected on different 2p-orbitals of the surface O atom. The panels in Fig. 4 demonstrate that the top of the upper valence band is formed predominantly by on-plane $2p_y$ orbitals of the surface O atom, in accord with plane-wave

calculations [4]. These orbitals are directed along the Ti–O–Ti bridge.

The lowest conduction band is flat between the Γ and X points. This looks very similar to the case of the bulk crystal. The DOS at the very bottom of conduction band contains contributions from *internal* Ti ions in the slab. The orbitals of the surface Ti ions contribute to the next lowest conduction bands at higher energy.

The indirect optical gap is reduced from 4.16 eV for the bulk down to 3.09 eV. The main contribution to this reduction comes from the split-off the surface valence band from internal valence bands at the M point. Surface valence and conduction bands are shifted up in energy, what is caused by a decrease of the electrostatic potential at the surface. As a result, the net electron density on the surface atoms is also reduced and the surface gets a positive charge.

Similar effects but with opposite sign are observed for the SrO-terminated slab (Figs. 2c and 5). The top of the upper valence band is still at the M point but now the upper band is formed from orbitals of internal O ions. The states located on the surface O ions essentially overlap in energy with the band of valence states. The conduction band created by orbitals of subsurface Ti ions is the lowest in energy conduction bands near the Γ point. Again, reduction of the indirect band gap stems mainly from a shift of the surface states, but from a shift of the surface conduction band. As a result, the band gap in the SrO-terminated slab becomes 3.71 eV. The electrostatic potential at the SrO-terminated surface increases, which causes lowering of energy of the surface bands, and an increase of the electronic density nearby the surface.

To our knowledge, there is the only UPS study [16] for the TiO_2- and SrO-terminated surfaces. The both spectra present two-peak structure in the valence band energy region, in the agreement with our calculations (see last windows in Figs. 4 and 5).

Summing up this Section, the band gap reduction for the TiO_2 termination is considerably larger than for the SrO termination. There is also a surprisingly large difference in the fine structures of the bulk and slab DOS. This, probably, can be explained by an influence of surfaces on positions of all bands in the thin slabs, which we used in our simulations. Dependencies of the band structure and DOS on the slab thickness should be still investigated in future.

4. Conclusions

At the M point of the surface Brillouin Zone we do observe (in accord with previous ab initio plane-wave calculations [4]) a split-off of the surface states from the valence band due to reduced electrostatic potential in the TiO_2-terminated surface and similar split-off the surface states from the conduction band at Γ point in the SrO-terminated surface. This effect, well known in ionic solids under the name of the *Tamm states*, could stimulate hole migration in the valence band or electrons in the conduction band (depending on the surface termination) to the surface and increase of its catalytic activity. However, there exist no deep-gap surface states, in accord with experiments [22] and recent ab initio calculations [4]. Note that B3LYP hybrid functional gives the optical gap for the bulk much closer to the experimental value than the DFT-LDA approach [4,10] which give a confidence to our surface gap results.

Our ab initio calculations indicate considerable increase of the Ti–O bond covalency near the surface, in agreement with the resonant photoemission experiments [15]. This should have impact on the electronic structure of surface defects (e.g., F centers), as well as affect an adsorption and surface diffusion of atoms and small molecules relevant in catalysis.

Lastly, our total DOS for the two terminations is in a qualitative agreement with the UPS [16]. However, the UPS spectra are not very informative, since they contain an uncontrolled mixture of surface and deeper-plane contributions. Much more informative is surface-sensitive metastable ion electron spectroscopy [23,24]. This gives the PDOS which could be directly compared with our calculations (Figs. 4 and 5).

Acknowledgements

This study was partly supported by European Center of Excellence in Advanced Material

Research and Technology in Riga, Latvia (contract # ICA-I-CT-2000-7007 to EK). Authors are indebted to A. Shluger, C. Pisani, A.M. Stoneham, and D. Vanderbilt for fruitful discussions.

References

[1] J.F. Scott, Ferroelectric Memories, Springer Verlag, Berlin, 2000.
[2] M.E. Lines, A.M. Glass, Principles and Applications of Ferroelectrics and Related Materials, Clarendon, Oxford, 1977.
[3] Proc. Williamsburg workshop on Fundamental Physics of Ferroelectrics-99, J. Phys. Chem. Sol. 61 (2) (2000).
[4] J. Padilla, D. Vanderbilt, Surf. Sci. 418 (1998) 64.
[5] J. Padilla, D. Vanderbilt, Phys. Rev. B 56 (1997) 1625.
[6] B. Meyer, J. Padilla, D. Vanderbilt, Faraday Discuss. 114 (1999) 395.
[7] F. Cora, C.R.A. Catlow, Faraday Discuss. 114 (1999) 421.
[8] R.E. Cohen, Ferroelectrics 194 (1997) 323.
[9] L. Fu, E. Yashenko, L. Resca, R. Resta, Phys. Rev. B 60 (1999) 2697.
[10] C. Cheng, K. Kunc, M.H. Lee, Phys. Rev. B 62 (2000) 10409.
[11] V. Ravikumar, D. Wolf, V.P. Dravid, Phys. Rev. Lett. 74 (1995) 960.
[12] S. Tinte, M.G. Stachiotti, in: R. Cohen (Ed.), AIP Conf. Proc. 535 (2000) 273.
[13] E. Heifets, E.A. Kotomin, J. Maier, Surf. Sci. 462 (2000) 19.
[14] E. Heifets, R.I. Eglitis, E.A. Kotomin, J. Maier, G. Borstel, Phys. Rev. B 64 (2001) 235417.
[15] R. Courths, B. Cord, H. Saalfeld, Solid State Commun. 70 (1989) 1047.
[16] T. Hikita, T. Hanada, M. Kudo, M. Kawai, Surf. Sci. 287/288 (1993) 377.
[17] M. Causa, A. Zupan, Chem. Phys. Lett. 220 (1994) 145.
[18] V.R. Saunders, R. Dovesi, C. Roetti, M. Causa, N.M. Harrison, R. Orlando, C.M. Zicovich-Wilson, Crystal-98 User Manual, University of Torino, 1999.
[19] P.W. Tasker, J. Phys. C: Solid State Phys. 12 (1979) 4977.
[20] J. Goniakowski, C. Noguera, Surf. Sci. 365 (1996) L657.
[21] V. Vikhnin, R. Eglitis, E.A. Kotomin, S. Kapphan, G. Borstel, Mater. Res. Soc. Symp. Proc. 677 (2001) AA4.15.1–AA4.15.6.
[22] R.A. Powell, W.F. Spicer, Phys. Rev. B 13 (1976) 2601.
[23] P. Stracke, S. Krischok, V. Kempter, Surf. Sci. 473 (2001) 86.
[24] V. Puchin, A.L. Shluger, J.P. Gale, E.A. Kotomin, J. Guenster, M. Brause, V. Kempter, Surf. Sci. 370 (1997) 190.